Immunity, Volume *56*

Supplemental information

M cell maturation and cDC activation determine the onset of adaptive immune priming in the neonatal Peyer's patch

Natalia Torow, Ronghui Li, Thomas Charles Adrian Hitch, Clemens Mingels, Shahed Al Bounny, Niels van Best, Eva-Lena Stange, Britta Simons, Tiago Maié, Lennart Rüttger, Narasimha Murthy Keshava Prasad Gubbi, Darryl Adelaide Abbott, Adam Benabid, Michael Gadermayr, Solveig Runge, Nicole Treichel, Dorit Merhof, Stephan Patrick Rosshart, Nico Jehmlich, Timothy Wesley Hand, Martin von Bergen, Felix Heymann, Oliver Pabst, Thomas Clavel, Frank Tacke, Hugues Lelouard, Ivan Gesteira Costa, and Mathias Walter Hornef

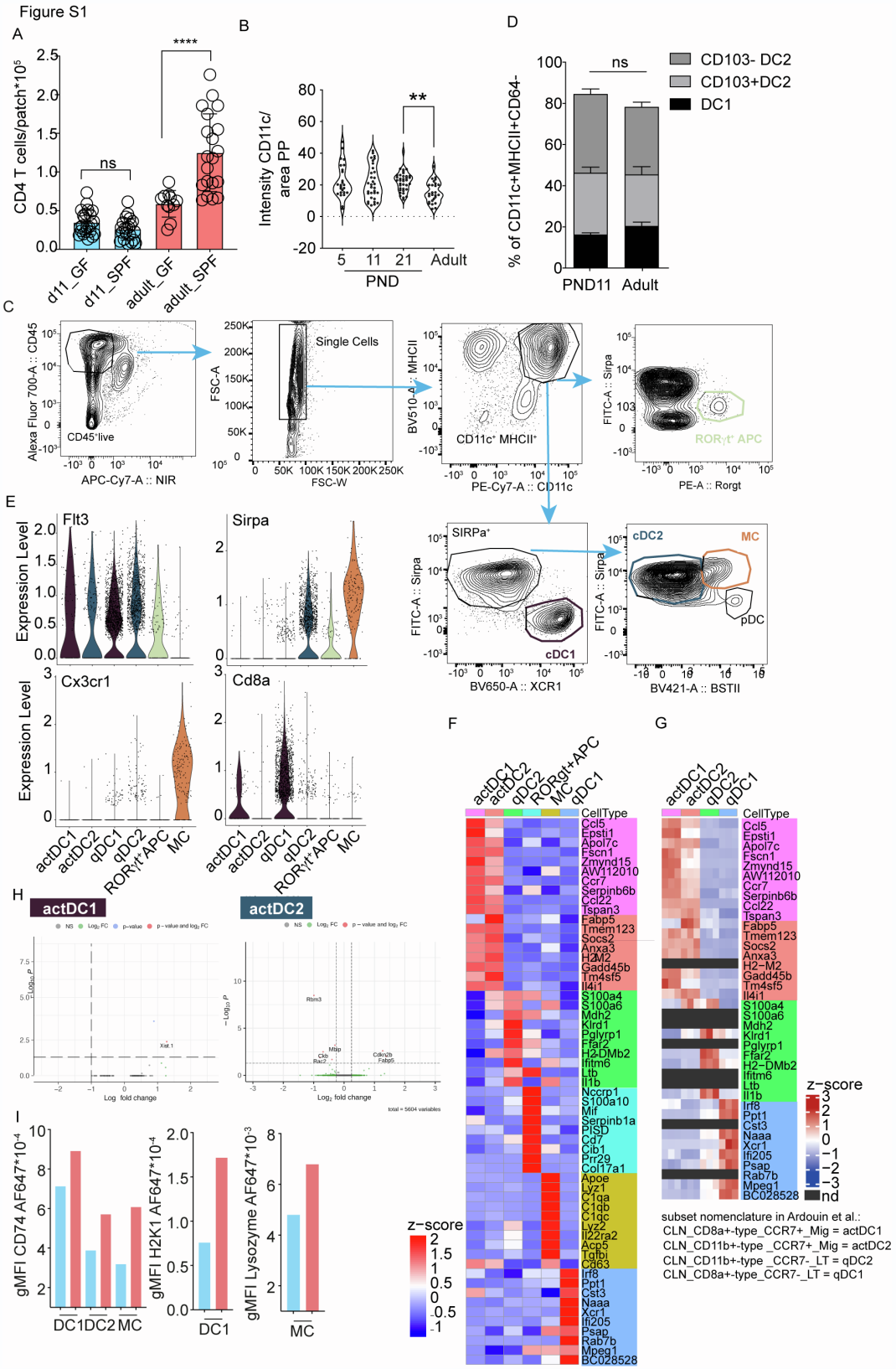

Supplementary Figure 1. Neonatal PP MNP exhibit diminished antimicrobial activity and reduced antigen processing and presentation capacity, related to Figure 1. (A) Number of CD4⁺ T cells per PP in postnatal day (PND) 11 (blue) and adult (red) specified pathogen free (SPF) and germ free (GF) mice (n=22-23 PP, mean+SD, Mann-Whitney U test). (B) Violin plot of the CD11c positive area normalized to the total PP area at the indicated postnatal age (PND) or in adult mice (n=25-36 follicles; 1-way-ANOVA, Kruskall-Wallis test). (C) FACS gating strategy to identify MNP subsets in PP. (D) Percentage of cDC1 (CD103⁺CD11b⁻ of CD64⁻CD11c⁺MHCII⁺CD45⁺live), CD103⁺ and CD103⁻ cDC2 (CD103⁺/⁻CD11b⁺ of CD64⁻ CD11c⁺MHCII⁺CD45⁺live) in the *lamina propria* of PND11 and adult mice (n=4, mean+SD, 1-way-ANOVA, Kruskall-Wallis test). (E) Expression levels of the indicated genes in the PP MNP subsets used for subset identification shown in the UMAP in Figure 1E. (F) Top DE genes defining the cell subsets in the UMAP in Figure 1E. (G) Expression of Top DE genes identified in (F) within the commonly differentially expressed genes in DC subsets from cLN detected by bulk RNAseq by Ardouin et al. (H) Volcano plots of between PND11 and adult mice differentially expressed (DE) genes in actDC1 (upper panel) and actDC2a (lower panel). (I) Mean fluorescence intensity (MFI) of the indicated antigen in PP cDC1, cDC2, and/or MC of PND11 (blue) and adult (red) mice (n=pooled litter/4 adult animals).

FIGURE S2

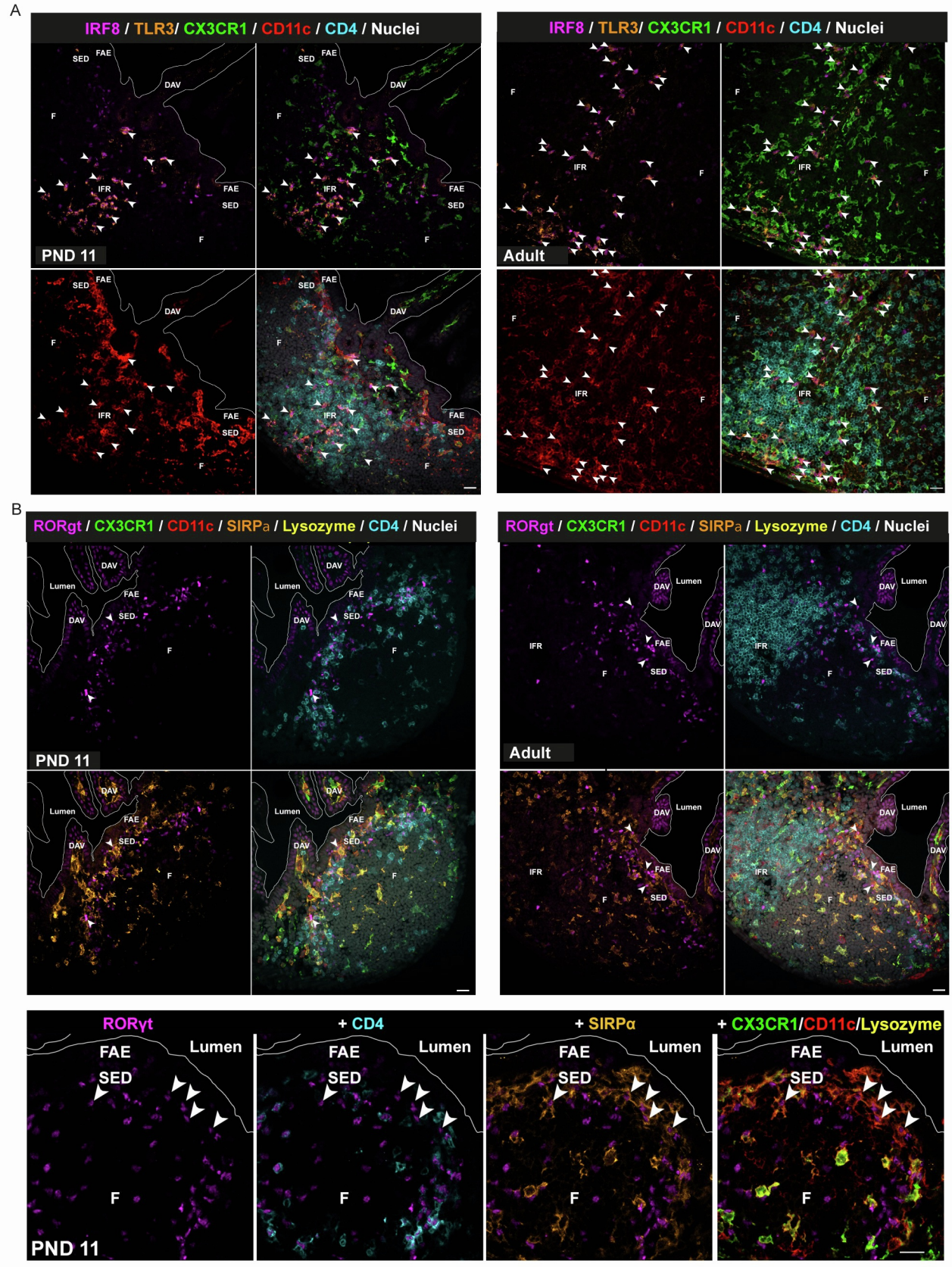

Supplementary Figure 2. Anatomical distribution of MNP in neonatal and adult PP, related to Figure 2. (A)+(B) Additional spectral confocal imaging projection representative of PND11 and adult PP from $CX_3CR1\text{-}GFP^{+/-}$ mice. Sections illustrate the anatomical distribution of (A) cDC1 using the markers TLR3, orange; IRF8, magenta; GFP, green; CD11c, red; CD4, blue (note that only TLR3 IRF8 double positive cells represent cDC1) and of (B) RORγt^{+} APC using the markers RORγt, magenta; GFP, green; CD11c, red; lysozyme, yellow; CD4, blue. Bars, 20 μm; FAE, follicle associated epithelium; SED, subepithelial dome; F, follicle; IFR, interfollicular region; DAV, dome associated villus.

FIGURE S3

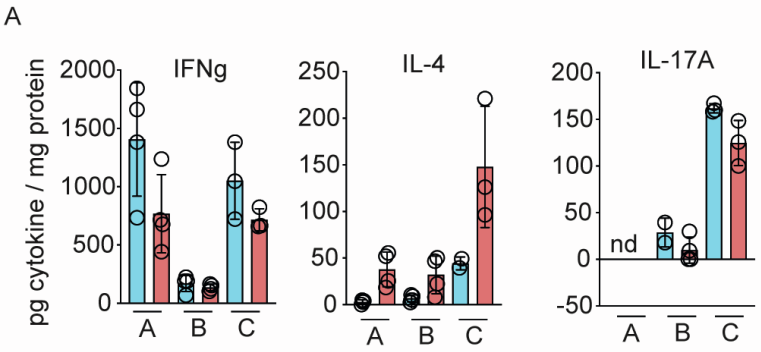

Supplementary Figure 3. Altered T cell priming by neonatal PP MNPs, related to Figure 3. (A) Independent experiments (A-C) showing T helper cytokine levels in the supernatant of 5-day co-cultures of OTII cells and MHCII^{+}CD11c^{+}CD45^{+}live MNP isolated from PP of PND11 (blue) and adult (red) mice in the presence of OVA shown for IFNg, IL-4 and IL-17A that were pooled after normalization in Figure 3C.

FIGURE S4

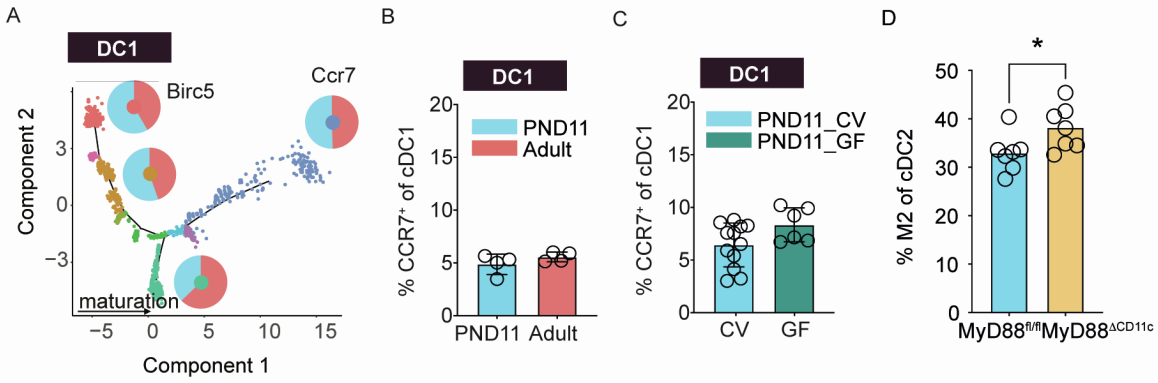

Supplementary Figure 4. Maturation delay of PP cDC subsets during the postnatal period, related to Figure 4. (A) Monocle pseudotime trajectory of cDC1 with relative contribution of adult (red) and PND11 (blue) cells to the indicated branches (left panel). (B and C) Percentage of CCR7^{+} cells among XCR1^{+}SIRPα^{-}MHCII^{+}CD11c^{+}CD45^{+}live cDC1 in (B) conventional PND11 (blue) vs. conventional adult (red) animals (n=4, mean) and (C) PND11 conventional (CV) vs. PND11 germ free (GF) animals (n=6-12, mean) determined by FACS. (D) Percentage of M2 (CD11b^{+}) cells among cDC2 (Mann-Whitney U test) in MyD88$^{\Delta CD11c}$ and MyD88$^{fl/fl}$ PND11 and adult mice (n=6-7).*, p<0.05; **, p<0.01; ***, p<0.001.

FIGURE S5

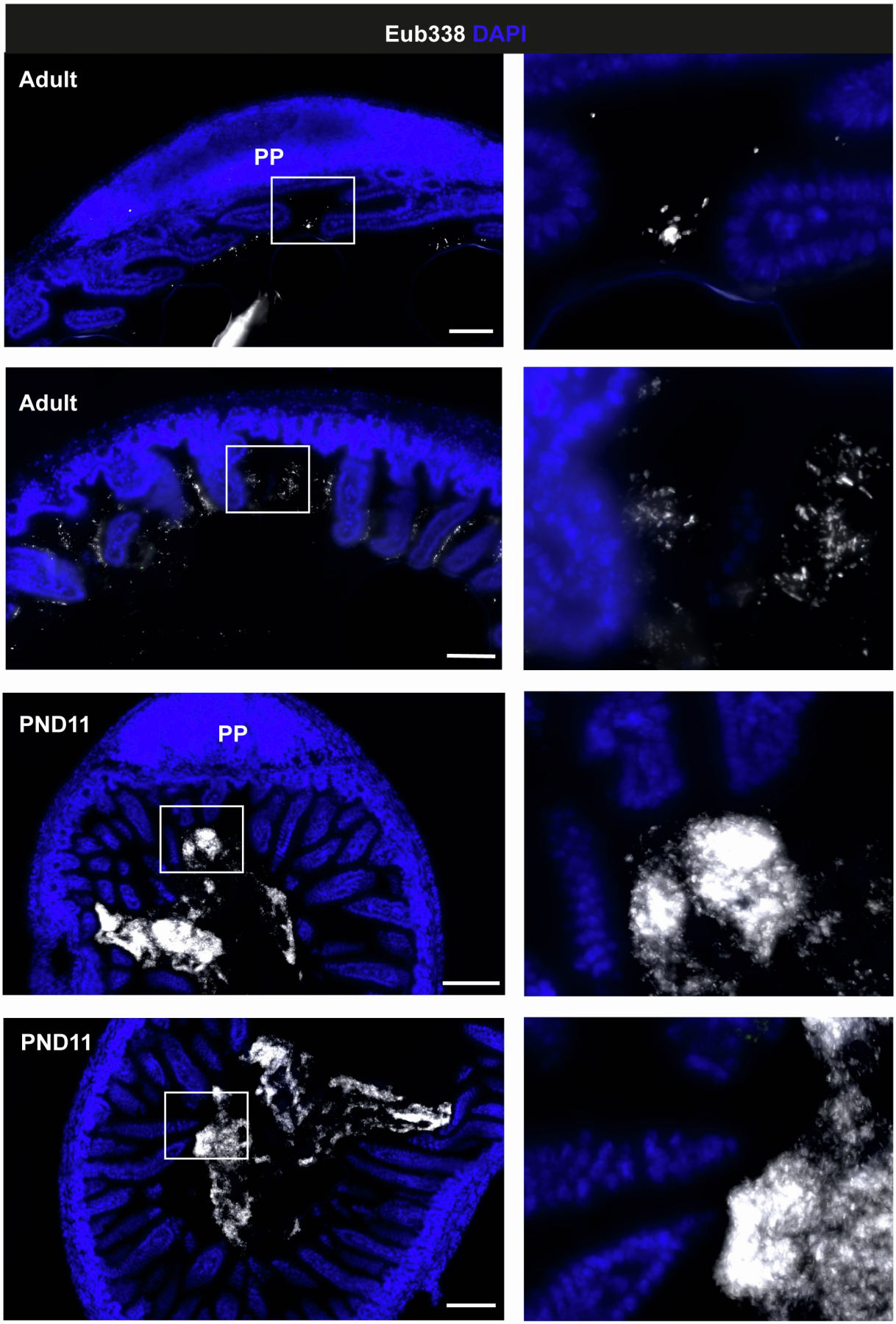

Supplementary Figure 5. Rapid postnatal establishment of a dense and immunogenic small intestinal core microbiome in the absence of adaptive immune maturation, related to Figure 5. (A) Immunofluorescence imaging representative of PND11 and adult SI (left) and PP (right) illustrating microbial colonization. Sections were stained with Eub333-AF647 (white) and DAPI (blue). Bars, 100μm.

FIGURE S6

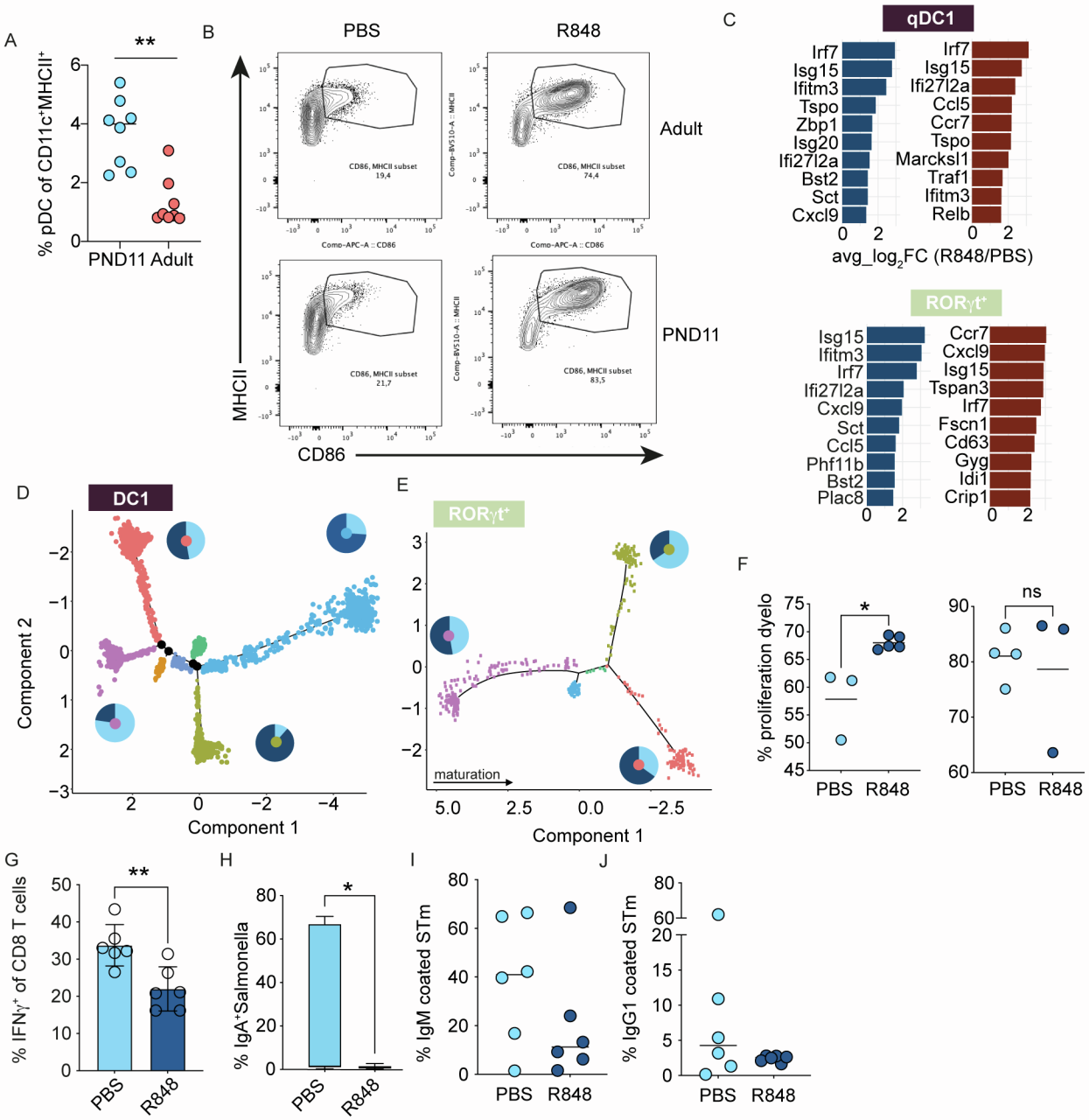

Supplementary Figure 6. IFN I induces DC activation in neonatal PP and modifies the adaptive immune response, related to Figure 6. (A) Percentage of BST2^{hi}SIRPα^{-}MHCII^{lo}CD11c^{+}CD45^{+}live pDC among MNP in PP of PND11 and adult mice (n=8, mean, Mann Whitney U test). (B) Representative FACS plots showing the percentage of CD86^{+}MHCII^{+} cells among MNP isolated from PP of PND11 (neonate) and adult mice 8h after oral gavage of 0.4 mg/g b.w. R848 or PBS. Percentage of (C) IgM^{+} and (D) IgG1^{+} *Salmonella* after incubation with sera from adult animals vaccinated against *Salmonella*±R848 as neonates (n=6, mean, Mann-Whitney U test). **, p<0.01. (C) Top 10 upregulated genes in PND11 (blue) and adult (berry) R848 vs. PBS qDC1 (upper panel) and RORγt^{+}APC (lower panel). (D)-(E) Pseudotime trajectory analysis of DC1 and RORγt^{+}APC from PND11 mice +/- R848, pie charts represent the relative contribution of cells from PBS (light) and R848 treated animals (dark) to the indicated branches. The branch with the highest S-score was set as the seed of the trajectory. (F) Percentage of proliferation dye diluted OTII cells in PP of neonatal mice 48h after oral gavage of OVA±R848 in two independent experiments. (G)-(K) Percentage of (G) IFNγ producing CD8 T cells, (H) anti-IgA^{+} *S.*Typhimurium (STm) incubated with small intestinal washes and serum (I) anti-IgM+ and (J) anti-IgG1+ STm from adult animals vaccinated with PAA STm±R848 as neonates (n=5-12; Box plot, Mann-Whitney U test).

FIGURE S7

A

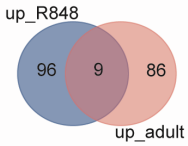

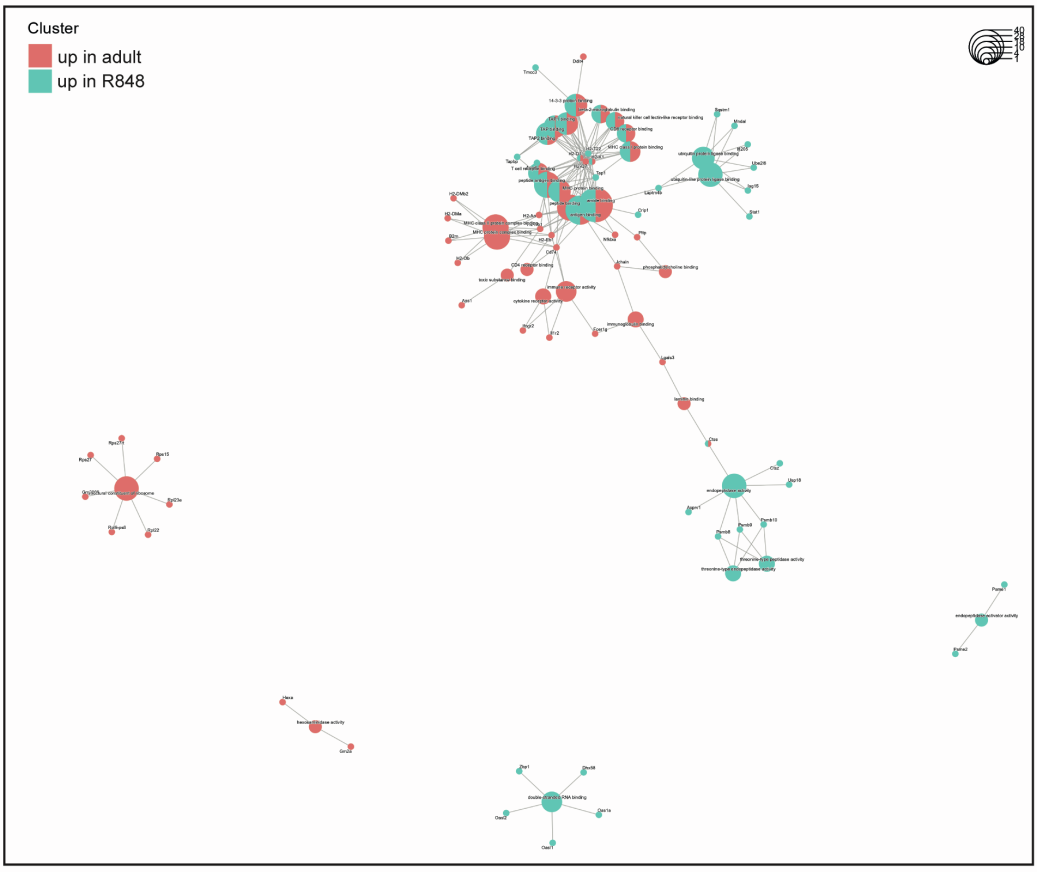

B

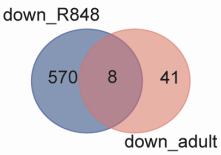

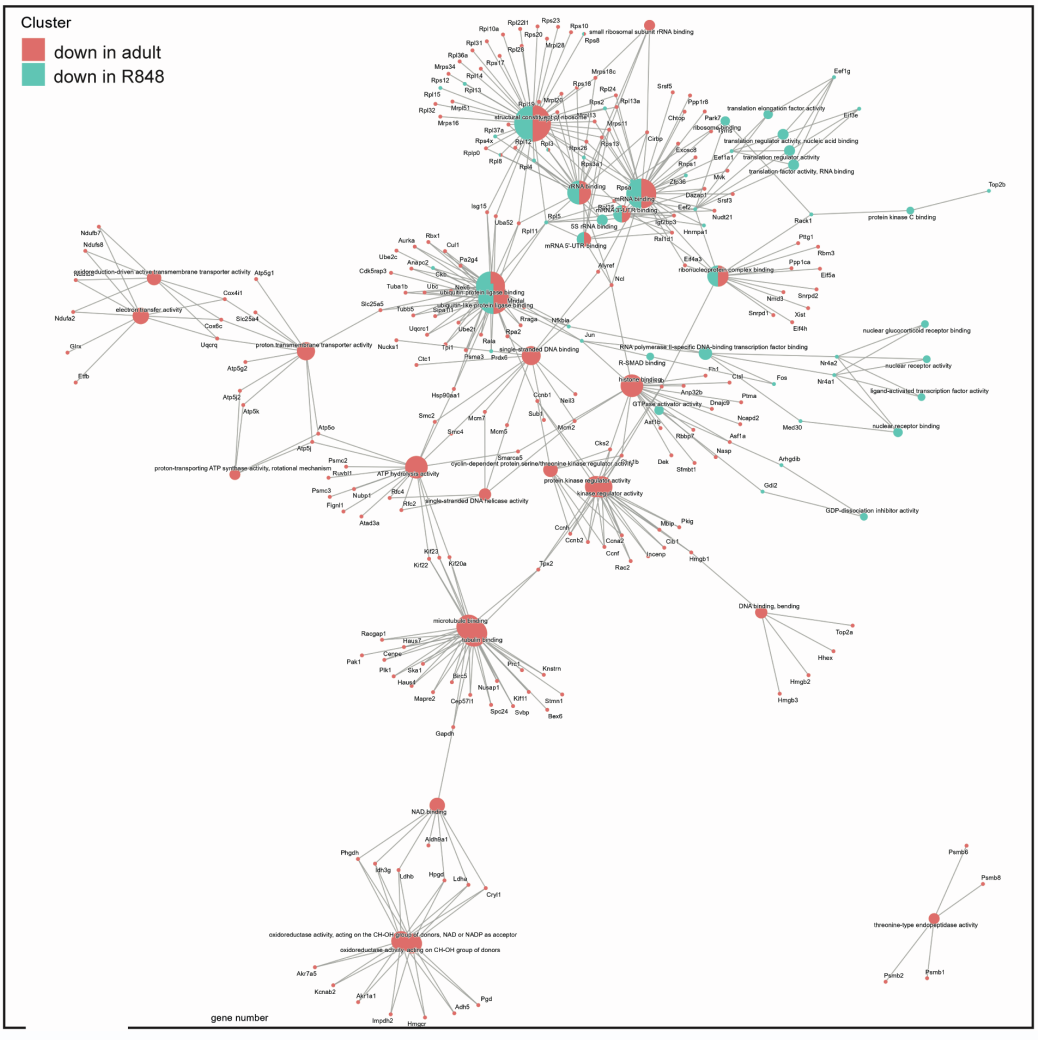

Supplementary Figure 7. Transcriptional changes after R848 do not mimic the neonatal to adult transition, related to Figure 5. (A) Venn diagram of DE genes (right panel) and cnet plot depicting GO terms (larger nods) and contributing genes (smaller nods) from genes upregulated in adult vs. neonatal and PND11 PBS vs. PND11 R848 qDC2. (B) Venn diagram of DE genes (right panel) and cnet plot depicting GO terms (larger nods) and contributing genes (smaller nods) from genes downregulated in adult vs. neonatal and PND11 PBS vs. PND11 R848 qDC2.